LEGIBILITY NOTICE

A major purpose of the Technical Information Center is to provide the broadest dissemination possible of information contained in DOE's Research and Development Reports to business, industry, the academic community, and federal, state and local governments.

Although a small portion of this report is not reproducible, it is being made available to expedite the availability of information on the research discussed herein.

CONF-8709152--2

Los Alamos National Laboratory is operated by the University of California for the United States Department of Energy under contract W-7405-ENG-36

TITLE: TRANSVERSE ENERGY DISTRIBUTION, CHARGED PARTICLE MULTIPLICITIES AND SPECTRA IN ^{16}O -- NUCLEUS COLLISIONS

LA-UR--87-3724

DE88 003176

AUTHOR(S): Jules W. Sunder

SUBMITTED TO: Proceedings of XVIII International Symposium on Multiparticle Dynamics, Tashkent, USSR, September 8-13, 1987

DISCLAIMER

MASTER

Los Alamos National Laboratory
Los Alamos, New Mexico 87545

TRANSVERSE ENERGY DISTRIBUTION, CHARGED PARTICLE MULTIPLICITIES AND SPECTRA IN ^{16}O - NUCLEUS COLLISIONS

The HELIOS Collaboration†

Presented by J.W. Sunier‡

1. INTRODUCTION

The HELIOS (High Energy Lepton and Ion Spectrometer) experiment, installed at the CERN Super Proton Synchrotron, proposes to examine in details the physical properties of a state of high energy created in nuclei by ultra-relativistic nucleus-nucleus collisions. It is generally believed that, at high densities or temperatures, a phase transition to a plasma of quark and gluons will occur. The dynamic of the expansion of such a plasma and its subsequent condensation into a hadron gas should markedly affect the composition and momentum distribution of the emerging particles and photons. The HELIOS experimental setup[1] therefore combines 4π calorimetric coverage with measurements of inclusive particle spectra, two particle correlations, low and high mass lepton pairs and photons. The emphasis is placed on transverse energy flow (E_T) measurements with good energy resolution, and the ability to trigger the acquisition of data in a variety of E_T ranges, thereby selecting the impact parameter or the violence of the collisions.

This short note presents HELIOS results, for the most part still preliminary, on ^{16}O - nucleus collisions at the incident energies of 60 and 200 GeV per nucleon. The E_T distributions from Al, Ag and W targets[2] are discussed and compared to the associated charged particle multiplicities from W. Charged particle and (converted) photon spectra measured with the external magnetic spectrometer are compared for ^{16}O + W and p + W collisions at 200 GeV per nucleon.

2. TRANSVERSE ENERGY DISTRIBUTIONS

The target region is surrounded by a box of calorimeter modules that cover the pseudorapidity interval $-0.1 < \eta < 2.9$. The forward region is covered by a beam calorimeter placed further downstream. The granularity of this calorimeter allows extension of the E_T measurement to the interval $2.9 < \eta < 4.9$. The E_T trigger is formed from appropriately weighted energy sums in the region $-0.1 < \eta < 2.9$, where the E_T resolution is $dE_T/E_T = 29\%\sqrt{E_T}$ (GeV), and the E_T scale has a systematic uncertainty of 7%. Data were recorded with W, Ag and Al targets. Runs with empty targets were also performed for the purpose of background subtractions, amounting to < 1% for $E_T > 50$ GeV. The ^{16}O component of the beam, 94% of the A/Z = 2 particle mixture hitting the targets, was isolated by dE/dx measurements. Data sets were obtained at the available beam energies of 60 and 200 GeV per nucleon.

The transverse energy cross-sections $d\sigma/dE_T$ are presented in Figure 1. For all targets and beam energies, the main feature of these distributions is a plateau region followed by a steeply falling slope. This behaviour is characteristic of the geometrical cross-section plotted as a function of the overlap integral over the areal nucleon densities of the two colliding nuclei. In this picture, the plateau region corresponds to peripheral collisions and the "knee" to the onset of central collisions, where the overlap is complete. To compare the different cross-sections, we define "$E_T^{central}$" as the value of E_T where the cross-section reaches a fraction of the plateau value. The fraction is chosen to be f=0.5 and the plateau value is defined as the cross-section for which the rate of change versus E_T is minimum. Figure 2 gives the beam energy and A dependence of $E_T^{central}$. Fits to the form A^x are shown, with $x = 0.48 \pm 0.02$ at 200 GeV per nucleon and $x = 0.43 \pm 0.02$ at 60 GeV per nucleon. At both incident beam energies, $E_T^{central}$ increases faster than the $A^{1/3}$ relation one might

† The names of the Collaboration members are omitted due to lack of space.

‡ Los Alamos National Laboratory, Physics Division, Los Alamos, New Mexico.

expect from the target nucleus thickness. The fact that the cross-section continues to rise indicates that the collisions procede in an energy regime well above the one where the projectile would fully stop in the target, even at 60 GeV per nucleon.

The similarity of the geometrical cross-section to the observed E_T distributions suggests a description of the data in terms of independent nucleon-nucleon collisions.[3] An effective number of collisions N is obtained by multiplying the geometrical overlap integral with the inelastic nucleon-nucleon cross-section. Assuming that the total E_T is Gaussian-distributed with a mean of $N\epsilon_0$ and a variance $\omega N\epsilon_0^2$, where ϵ_0 and ω are adjustable parameters, one obtains excellent fits to the data,[4] as indicated in Figure 1. The values of ϵ_0 are $\approx$ 1 GeV and compare well with the mean transverse energy of $\approx$ 1.4 GeV measured in p-p collisions at $\sqrt{S}$ = 20 GeV.

3. CHARGED PARTICLE MULTIPLICITIES

The charged particle multiplicities have been measured with a silicon pad and a silicon ring detector. The pad detector has 400 segments, lies 9 cm behind the target, and covers the region $2.5 < \eta < 5.0$. The ring detector is 3 cm downstream from the target and, with 384 segments forming 32 rings approximately equally spaced in pseudorapidity, covers the region $0.9 < \eta < 2.8$. The multiplicity increases linearly with E_T. Assuming that 55% of E_T is produced by charged particles, as inferred from pp collisions and HIJET, one calculates the average p_T per charged particle plotted as a function of E_T in Figure 3. The data indicate an average p_T of $\approx$ 340 MeV, and suggest a slight (7%) increase with E_T. The charged particle multiplicity distribution as a function of pseudorapidity is shown in Figure 4, together with the measured distribution of $dE_T/d\eta$, for central collisions at 200 GeV per nucleon. The multiplicity data complement the E_T measurements, particularly in the region $\eta > 2.9$, where the granularity of the calorimeter is very coarse. The experimental rapidity distributions peak at a value of η close to η (c.m) = 2.45 characteristic of a system of 16 Oxygen nucleons interacting with 50 nucleons of the target, assuming full stopping. We note that the highest E_T measured in ^{16}O-W collisions at 200 GeV per nucleon corresponds to $\approx$70% of the kinematic limit of such a system. Also shown in Figure 4 are the $dE_T/d\eta$ predictions based on the dual parton model IRIS.[5] The quantitative agreement with the measured $dE_T/d\eta$ is quite good, with some possible underestimation in the region $\eta < 1$. The multiplicity distribution also peaks at a lower value of η than the IRIS generated $dE_T/d\eta$.

4. EXTERNAL SPECTROMETER RESULTS

4.1. Charged particle spectra

The external spectrometer views the target through a narrow slit in the calorimeter wall, covering the pseudorapidity intervall $0.9 < \eta < 2.0$. A magnet with a p_T kick of $\approx$ 70 MeV/c and two high resolution (150 μm) drift chambers provide the momentum measurement of charged particles. Particle identification is achieved by a combination of time of flight and Cherenkov counters. Figure 5 shows a comparison of the p_T distribution of negative tracks (π^-) from ^{16}O - W and p - W collisions at 200 GeV per nucleon. Over four orders of magnitude these spectra are identical, and show the canonical slope characteristic of p-p collisions. The flattening high momentum tail of the spectra has not yet been corrected for finite resolution effects nor for particle decays between the two drift chambers of the spectrometer. In Figure 6, we show the average p_T for identified protons and π as a function of E_T, for the reaction ^{16}O - W at 200 GeV per nucleon. A momentum cut of $p^* < 2$ GeV/c has been applied to avoid p, π confusions and minimise the effect of the flat background attributed to particle decay. These data agree well with the results of Figure 4 and attribute to protons the observed rise of $< p_T >$ with E_T. We note that the data are not yet corrected for the slightly different spectrometer acceptance for positive and negative particles. This is reflected by the different values for π^+ and π^- data.

4.2. Photon spectra

A converter, 5% in radiation length, is placed directly upstream from the first drift chamber of the spectrometer, to allow the measurement of photons by tracking the converted electron-positron pairs. Two planes of multiwire proportional counters bracket the converter and localise the conversion point. In Figure 7, we compare the p_T distributions of photons from the ^{16}O - W and p - W reactions at 200 GeV per nucleon. Here again, the two spectra are identical within errors. The direct photon contribution to these spectra will be extracted after subtraction of the dominant π_0 contribution, process that will require a very precise determination of the charged pion spectra.

5. CONCLUSION

The data presented can largely be explained by convolution of multiple independent nucleon-nucleon collisions. The E_T distributions indicate a partial stopping regime. The charged particle multiplicity increases linearly with E_T. A slight increase of the average charged particle $< p_t >$ with E_T is observed. Particle identified spectra attribute this rise to protons. The p_T distributions of pions and photons are the same for p-W and ^{16}O-W reactions, within experimental uncertainties.

REFERENCES

1. H. Gordon *et al.*, HELIOS experiment proposal, CERN SPSC/84-43/P203 (1984), SPSC/85-74/M241 (1985).

2. T. Akesson *et al.*, CERN-EP/87-176 (1987), submitted for publication in Z. Phys. C.

3. G. Baym, P. Braun-Munsinger and V. Ruuskanen, Phys. Lett. B190, 29 (1987). A. D. Jackson and H. Boggild, Nucl. Phys. A470, 609 (1987).

4. H. H. Thodberg, internal HELIOS Note 219 (1987).

5. J. P. Pansart, Nucl. Phys. A461, 521c (1987).

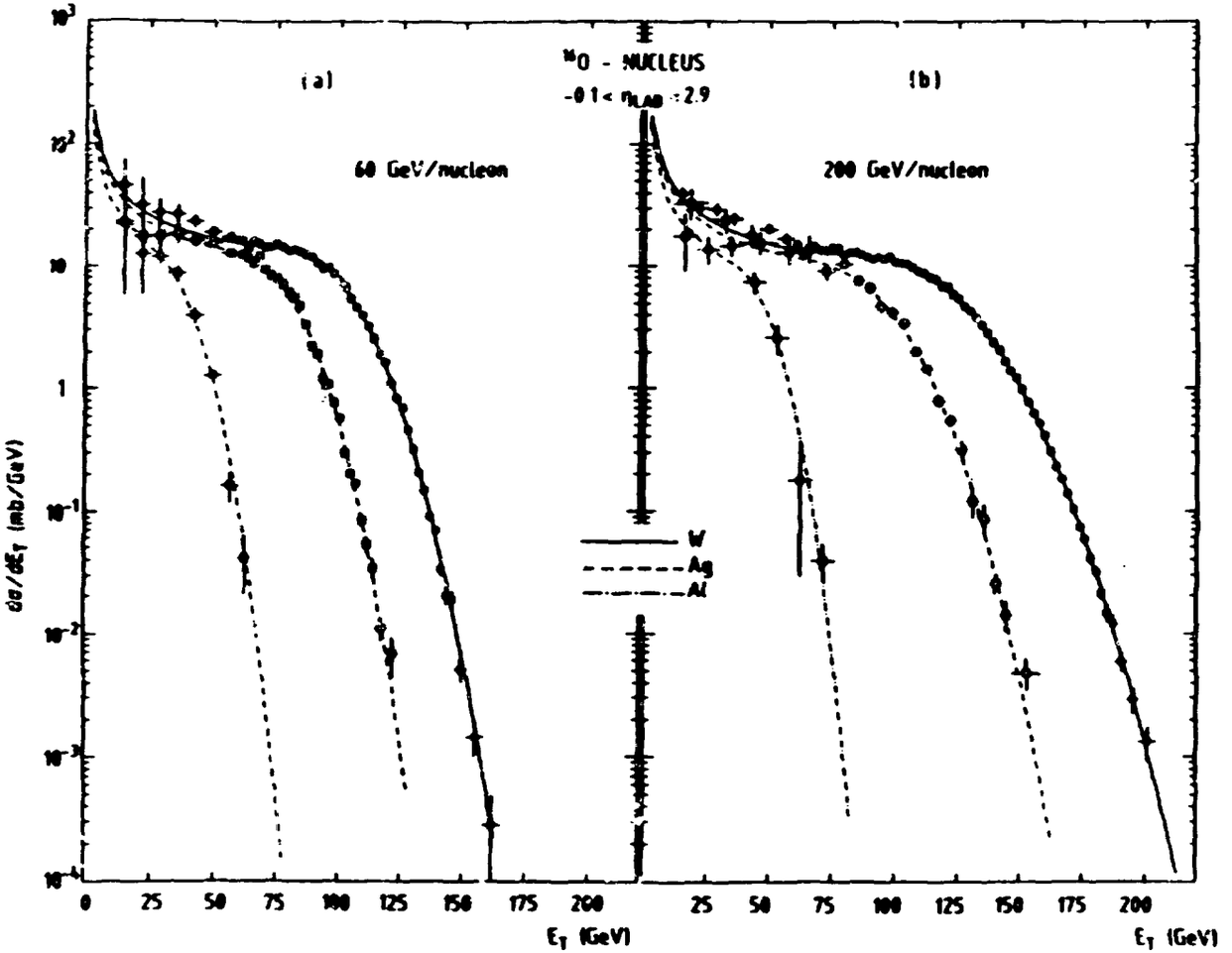

Fig. 1. The E_T cross-section for ^{16}O beam at a) 60 GeV per nucleon and b) 200 GeV per nucleon on W, Ag and Al targets. The E_T is measured in the region $-0.1 < \eta < 2.9$. The curves are the results of geometrical parametrisation fits.

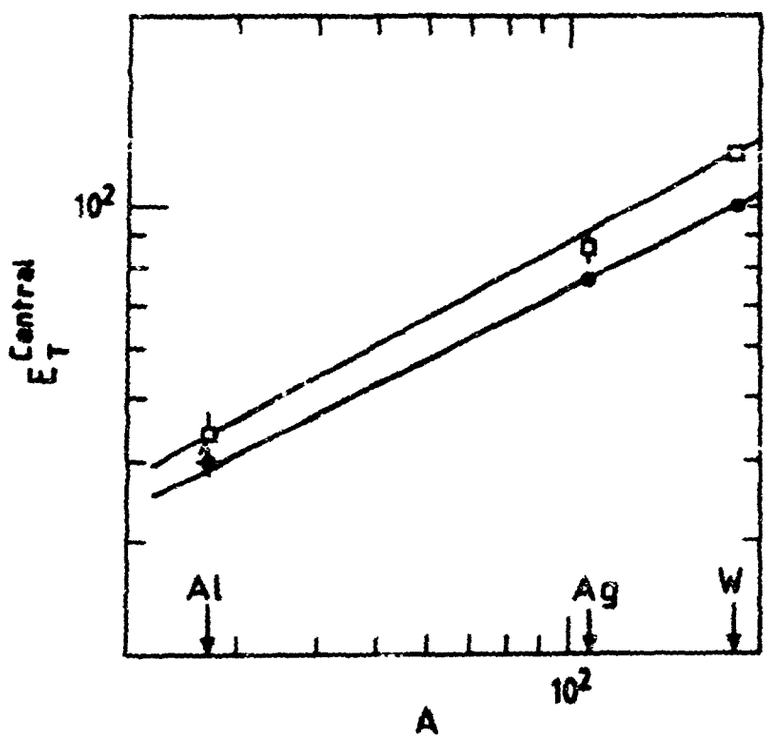

Fig. 2. E_T of average central collisions versus the atomic mass number A of the targets for 60 (lower) and 200 (upper) GeV per nucleon incident energies.

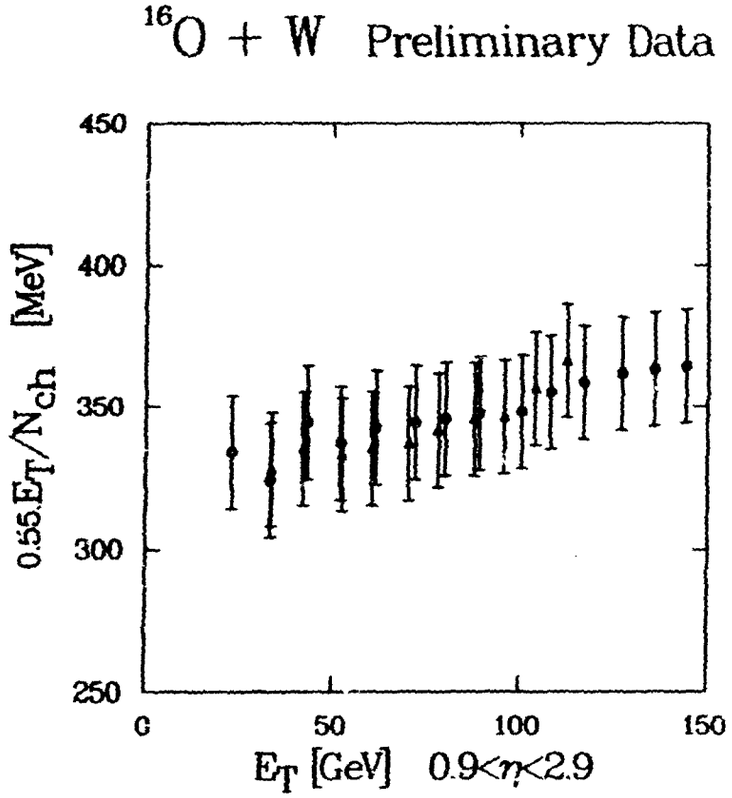

Fig. 3. Average charged particle p_T versus E_T for 60 (triangles) and 200 (circles) GeV per nucleon incident energies.

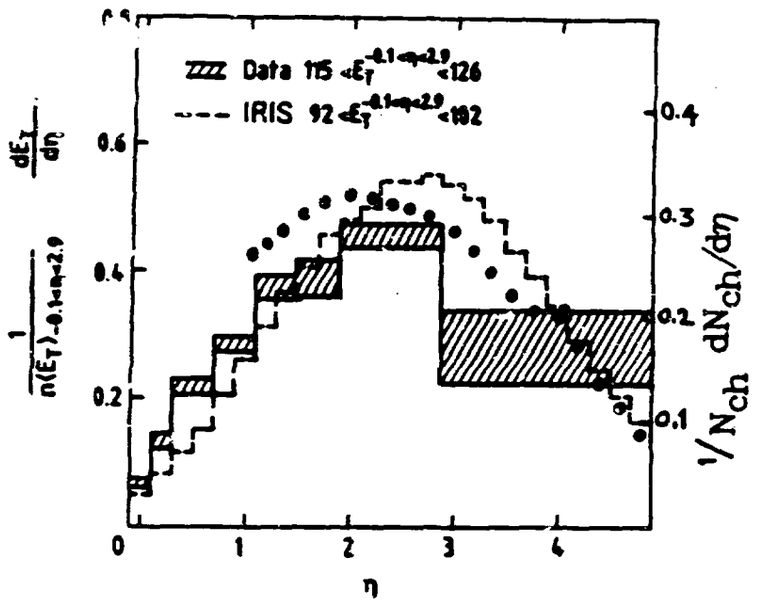

Fig. 4. Comparison of pseudorapidity distributions of central ^{16}O-W collisions at 200 GeV per nucleon: a) $dE_T/d\eta$ data (solid line) and its IRIS prediction (dotted line) and b) Charged particle multiplicity $dN_{ch}/d\eta$ (dots)

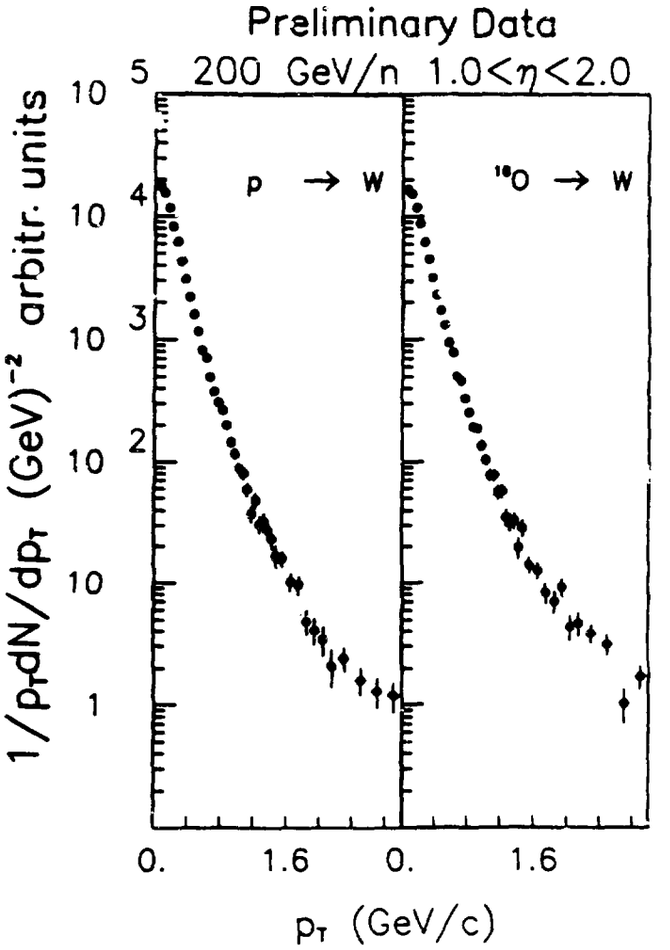

Fig. 5. The Lorents invariant p_T spectra of all negative particles (π^-) for p-W and ^{16}O-W collisions at 200 GeV per nucleon.

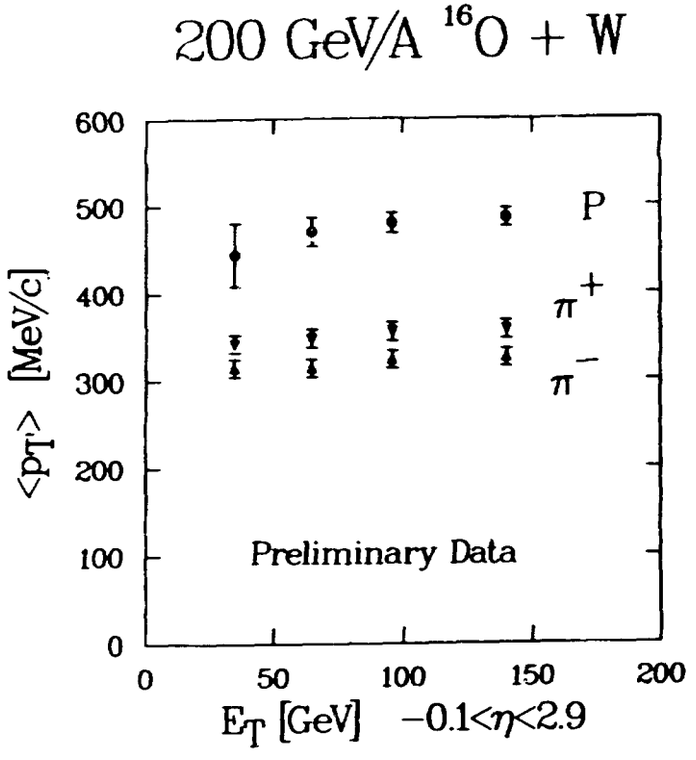

Fig. 6. The average p_T per particle as a function of E_T for protons, π^+ and π^-, with a cutoff of $p < 2$ GeV/c. Note that π^+ and π^- data have not been corrected for differences in spectrometer acceptance.

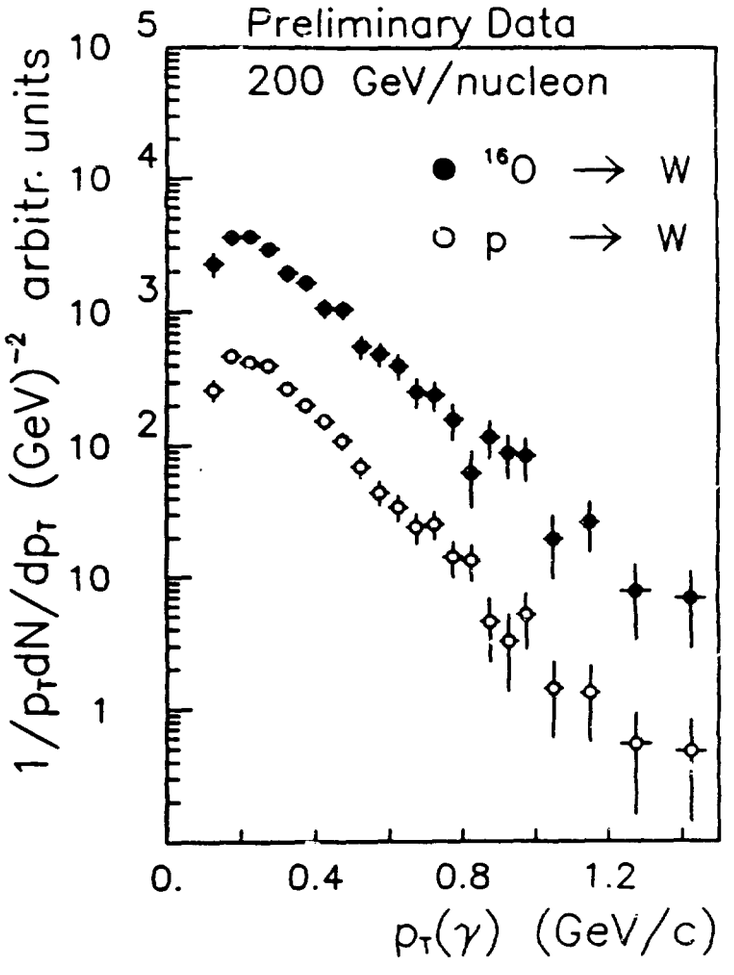

Fig. 7. The photon p_T spectra for p-W and ^{16}O-W collisions at 200 GeV per nucleon.